J Sol-Gel Sci Technol (2013) 68:60–66
DOI 10.1007/s10971-013-3134-2

ORIGINAL PAPER

Enzyme mediated synthesis of Ag–TiO_2 photocatalyst for visible light degradation of reactive dye from aqueous solution

V. Gunasekar · B. Divya · K. Brinda · J. Vijaykrishnan · V. Ponnusami · K. S. Rajan

Received: 30 April 2013 / Accepted: 30 July 2013 / Published online: 8 August 2013

Abstract The purpose of this study was to develop bio-inspired photocatalyst with solar light activity for textile dye degradation. Three TiO_2 samples namely TiO_2 (TiO_2-A), biotemplated TiO_2 (TiO_2-B), and enzyme mediated Ag–TiO_2 biotemplate (TiO_2-C), were developed. The presence of anatase phase of TiO_2 and silver in synthesized samples were confirmed using X-ray diffraction, field emission scanning electron microscopy, energy-dispersive spectroscopy, and UV–Vis–NIR spectroscopy. Photocatalytic efficiencies of these photocatalysts were evaluated by studying the oxidation of a commercial reactive dye (reactive black) under solar light irradiation in batch reactors. Photocatalytic efficiencies of the sample were compared using statistical tools like one-way ANOVA and Tukey test. The results confirmed that photocatalytic efficiency of TiO_2-C was 40 % higher than that of TiO_2-A under solar light irradiation.

Keywords Visible light photocatalyst · TiO_2 · Biotemplate · Textile dye · Nanoparticles

1 Introduction

Bio-inspired synthesis of highly intricate hierarchical structures using biological materials as templates or precursors is one of the interesting areas of green technology. Materials synthesized by such techniques have found their application in different fields like optics, electronics, biomedical and environmental technology [1–3]. In the recent past, many researchers have attempted to develop materials through green synthesis to solve various environmental problems. Pollution due to growth of industries is one the major problems faced by developing countries. Dyes are complex synthetic molecules that are major constituents of the industrial effluent streams of paint, textile and leather industries. Even small amount of these dyes in water bodies affects the biotic and abiotic factors in the ecosystem [4–6]. Various physico-chemical methods like adsorption, coagulation, ion-exchange, biodegradation etc., are available for decolorization of textile waste water [4, 6–10]. Among all these processes, photocatalytic oxidation appears to be more attractive [11–13]. The major advantages of photocatalytic oxidation over other physico-chemical methods are (1) complete mineralization of dyes (2) no sludge generation and (3) mild reaction conditions. Thus, application of photocatalysts for the elimination of organic pollutants from industrial effluents has been one of the most interesting areas of research.

In a semiconductor photocatalyst, photo irradiation causes excitation of electrons from valance band to the conduction band. This results in the formation of electron–hole pairs which are responsible for degradation of the dyes. Reactive intermediates formed by the reaction of OH radical with hole and intermediates formed due to water splitting reactions leads to mineralization of dye molecules [14–16]. In particular, TiO_2 has been widely used in wastewater treatment because of its inert nature, stability, low-cost and resistance to photo-corrosion [17, 18]. However the major weakness of TiO_2, as a photocatalyst, is that it requires UV light source and it absorbs only a small fraction of solar light. When TiO_2 absorbs photons with

V. Gunasekar · B. Divya · K. Brinda · J. Vijaykrishnan · V. Ponnusami (✉)
School of Chemical and Biotechnology, SASTRA University, Thirumalaisamudram, Thanjavur 613 401, Tamil Nadu, India
e-mail: vponnu@chem.sastra.edu; ponnusamiv@gmail.com

K. S. Rajan
Centre for Nanotechnology and Advanced Biomaterials, SASTRA University, Thanjavur 613 401, Tamil Nadu, India

energy greater than or equal to its band gap energy, electrons in its valance band are excited and jump to conduction band thereby generating electron–hole pairs. The holes can either oxidize organic pollutants or produce reactive oxygen species like ·OH. When this process takes place in the presence of oxygen, super-oxide anions ($O_2^{\cdot-}$) are produced. Photocatalytic performance of TiO_2 is influenced by its crystallite size, surface area and dopants [19, 20]. Doping TiO_2 with transition metals, like Ag, Fe, Mo, Ru, Os, Re and V improves photocatalytic efficiency of TiO_2 by improving its visible light absorbance [12, 18, 21–23]. Transition metal doping of TiO_2 results in formation of band gap traps and prevents recombination of electrons from conduction band or holes from valance band.

Nanoporous TiO_2 is synthesized by several methods including, chemical vapor deposition (CVD), sol–gel, and hydro-thermal method. In the recent past, template assisted synthesis of TiO_2 had been studied extensively and it had been shown that template controlled syntheses produce excellent surface morphological characteristics and result in enhanced catalytic efficiency [17, 24]. However, conventional templating methods are generally expensive, energy intensive and not eco-friendly. Thus, several scientists across the globe are investigating development of bio-inspired catalysts through green synthesis technology. Major strength of utilizing biological materials as templates in green synthesis is that, they are environmentally benign and the synthesized particles have controlled structural design and morphology. Several biomaterials like wood, egg shell, butterfly wings, plant materials, etc. [25, 26] have been employed as biotemplates in nanomaterial synthesis.

In this paper, we investigate a novel single step method for the synthesis of TiO_2 using *E. coli* as biotemplate with simultaneous in situ silver incorporation. Enzyme nitrate reductase reduces silver ions in silver nitrate solution to metallic silver [27, 28]. *E. coli* was choosen in this study as it is capable of producing nitrate reductase enzyme which is required for this study. To the best of our knowledge, this is the first report on enzyme mediated synthesis of Ag–TiO_2 using *E. coli as* biotemplate.

2 Experimental section

2.1 Materials

Analytical grade isopropyl alcohol (Merck), titanium (IV) isopropoxide (97 %, Sigma–Aldrich), and silver nitrate (Himedia) were used in this study without further purification. Reactive black B dye (C.I. 20505) was purchased from Indian Dyes and Chemicals, Tirupur, Tamilnadu, India. *E. coli* (MTCC 448) culture was grown on nutrient agar (Beef Extract 1.0 g/l, Yeast Extract 2.0 g/l, Peptone 5.0 g/l, NaCl 5.0 g/l, Agar 15.0 g/l). The culture was cultivated at 37 °C in LB broth containing Tryptone 10 g/l, Yeast extract 5 g/l and NaCl 5 g/l at 200 rpm in a rotary shaker.

2.2 Methods

2.2.1 Synthesis of TiO_2 (TiO_2-A)

The TiO_2 precursor, titanium (IV) isopropoxide (2 ml), was dissolved in isopropyl alcohol (100 ml) and kept under stirring for 2 h. The solution was centrifuged at 10,000 rpm for 10 min and TiO_2 pellets were collected. The TiO_2 pellets were then calcined in a muffle furnace at 550 °C for 1 h. Calcined TiO_2 was ground finely and stored for further use. This as prepared TiO_2 was labeled as TiO_2-A.

2.2.2 Synthesis of biotemplated TiO_2 (TiO_2-B)

E. coli cells grown in Luria–Bertani (LB) broth were isolated by centrifugation at 6,000 rpm for 10 min. The harvested cells were re-suspended in 100 ml of isopropyl alcohol and stirred well for 30 min. 2 ml of titanium (IV) isopropoxide was added to this mixture drop-wise and the mixture was stirred for 2 h. Biotemplated TiO_2 particles were separated from the mixture by centrifugation and then calcined at 550 °C for 1 h. This product was labeled as TiO_2-B.

2.2.3 Synthesis of biotemplated Ag–TiO_2 (TiO_2-C)

Silver nitrate (0.5 M) solution 1–5 mol% was added to 200 ml of 20 h *E. coli* culture grown in LB broth. The culture with silver nitrate was agitated at 200 rpm for 30 min in an orbital shaker and then centrifuged at 10,000 rpm for 10 min. The pellets, cells loaded with silver, were used as biotemplates for TiO_2 synthesis. The pellet was then re-suspended in isopropyl alcohol (100 ml) and 2 ml of titanium (IV) isopropoxide was added drop-wise. The mixture was then stirred for 2 h. The precipitate was then calcined at 550 °C for 1 h and finely ground for further use. The Ag–TiO_2 samples thus synthesized with 1, 2, 3, 4 and 5 percentage of $AgNO_3$ solution were labeled as TiO_2-C1, TiO_2-C2, TiO_2-C3, TiO_2-C4 and TiO_2-C5 respectively.

2.2.4 Analysis

X-ray diffraction (XRD) pattern was recorded by irradiating the samples with Cu-Kα, analyzed at an angle 2θ and scan rate of 0.01 °/s using Bruker D8 X-ray diffractometer, Germany. The samples were pelletized at a pressure of 25 ton and analyzed for their elemental composition using S8 Tiger X-ray fluorescence (XRF) spectrometer, Bruker

AXS, Germany. The optical spectra for the samples were obtained using Perkin-Elmer Lamda75 UV–Vis–NIR spectrophotometer. The morphology and elemental composition were analyzed by a cold field emission scanning electron microscope (FE-SEM, JSM 6701F, JEOL, Japan). Surface area (BET) and pore size distribution of the catalysts were determined by nitrogen gas adsorption method at 77.3 K using accelerated surface area and porosimetry system (ASAP 2020 V3.04 H, Micromeritics, USA).

2.2.5 Photocatalytic studies

The photocatalytic activities of synthesized materials were investigated by studying the degradation of a commercial dye, Reactive Black, under solar irradiation. 0.1 g TiO_2 sample was added to 100 ml of 100 ppm reactive black dye solution and stirred for 20 min in dark. The mixture was then placed under sunlight and samples were drawn from the mixture at regular time intervals. Percentage decolorization was calculated from the optical density of dye solution recorded using Systronics UV–visible spectrophotometer 2201. Optical density of the sample was measured at the characteristic wavelength of reactive black dye (580 nm) corresponding to its maximum absorbance. All experiments were done in duplicates and the photocatalytic efficiencies of the samples were investigated statistically using Minitab 16 software. One-way ANOVA and Tukey's test were performed to test the statistical significance between different TiO_2 catalysts.

3 Results and discussion

3.1 Mechanism of enzyme mediated synthesis of *E. coli* templated Ag–TiO_2

E. coli cells grown in LB broth were harvested during the stationary phase for the synthesis of biotemplated Ag–TiO_2. As mentioned in Sect. 2.2.3 the harvested culture was centrifuged and the collected cells were re-suspended in isopropyl alcohol. Silver nitrate was added to *E. coli* cells collected during stationary phase (20 h). *E. coli* cells secrete enzymes required for the reduction of silver nitrate. Sigma factors (protein) in *E. coli* transcribe *rpo*S genes at the end of exponential phase into RpoS, regulatory gene for stationary phase [27]. RpoS genes respond to environmental stresses like osmotic shock, acidity, low temperature, UV exposure, nutrient limitation, etc. In order to manage the shortage of growth nutrients and minerals at the beginning of stationary phase, RpoS activity increases and induces the production of nitrate reductase enzyme in *E. coli* [27]. These enzymes are responsible for the reduction of silver ions in silver nitrate solution and silver nanoparticles are synthesized. At this stage, TiO_2 precursor was added to the solution under constant stirring. TiO_2, along with silver, precipitated on the internal and external surface of the cells. The precipitate was then collected and calcined at 550 °C to get biotemplated Ag–TiO_2.

3.2 Characterization

X-ray diffraction studies were performed in order to confirm the presence of TiO_2 and silver in its crystalline phase (Fig. 1). Relative crystallinity and the phase structure of the samples were confirmed by comparing the patterns with joint committee on powder diffraction standards (JCPDS) files for TiO_2 and silver. Presence of anatase phase in the synthesized materials was identified from diffraction peaks at 25.6°, 37.9°, 48.3° and 54.2°. The 2θ values from these peaks correspond to the reflections from (1 0 1), (0 0 4), (2 0 0) and (1 0 5) planes (JCPDS No. 21-1272) [29]. Diffraction peaks at 38.1° and 44.3° as a response of reflection from (1 1 1) and (2 0 0) planes (JCPDS No. 4-783) [30] were sharp and strong in TiO_2-C. This observation confirmed the presence of silver in TiO_2-C and suggested that the product obtained was possibly a nanocomposite. Broader and less intense peaks of TiO_2-A confirmed that the particles were smaller in size and amorphous in nature. The crystallite size was calculated using Debye–Scherrer formula (Eq. 1) and listed in Table 1. Since the enzymatic reduction is quite faster, silver nanoparticles are formed on the surface of TiO_2 resulting in nanocomposites.

$$D = \frac{k\lambda}{\beta \cos\theta} \tag{1}$$

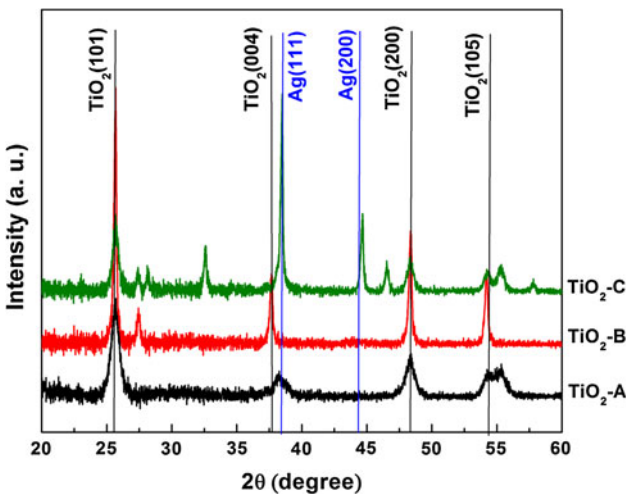

Fig. 1 X-ray diffraction patterns of TiO_2-A, TiO_2-B and TiO_2-C. The peaks of pure TiO_2 (*black thin line*) and Ag (*blue thick line*) were shown as *vertical lines* (Color figure online)

Table 1 Particle size analysis

Samples	2θ (degree)		Full width at half maximum	Crystallite size (nm) XRD	Grain size (nm) SEM	BET surface area (m^2/g)
	TiO_2	Ag				
TiO_2-A	25.6	–	0.730	11	35	18.63
TiO_2-B	25.6	–	0.212	38	51	34.15
TiO_2-C	25.6	37.8	0.230, 0.189	39.5	81	30.47

where $k = 0.89$ (constant), λ = wavelength of X-ray (1.5406 Å), β = corrected peak broadening (full width at half maximum) and θ = diffraction angle (degree).

Presence of silver (10.22 %) in TiO_2-C samples was also confirmed from the XRF elemental analysis. Traces of sodium, chlorine and potassium (0.04–0.94 %) were also observed in the samples TiO_2-B and TiO_2-C. The absorbance spectra recorded between 250 and 800 nm using UV–Vis–NIR spectrophotometer for all TiO_2 samples and are shown in Fig. 2. Light absorbance in the visible range was maximum for TiO_2-C among the three samples tested and is in the following order TiO_2-C > TiO_2-B > TiO_2-A. TiO_2-C exhibited a wide absorption spectrum in the range of 400–800 nm with maximum absorbance at 600 nm. This phenomenon was ascribed to surface plasmon resonance of Ag present in TiO_2-C [31]. This observation was consistent with the XRD results discussed above.

Scanning electron micrograph and its corresponding energy-dispersive X-ray analysis for the TiO_2 samples are shown in Fig. 3. The morphologies of the samples are depicted in SEM images with average grain size of the TiO_2 samples were in the range of 35–85 nm. The samples appeared as clusters of nano-sized structures formed by nucleation and subsequent crystal growth. Biotemplated materials (TiO_2-B) and (TiO_2-C) were found to be more porous as compared to as prepared sample (TiO_2-A). This may be due to the fact that TiO_2 and Ag precursors penetrated deep inside the *E. coli* cells and utilized cell and its organelles as template. Primary particle formation started in supersaturated solution after reaching the metastable zone and then increased in size with crystal growth i.e., nucleation started at room temperature. Presence of silver and nitrate ions, coarsing time and temperature are the major parameters that decide the size of primary particle. Higher temperature

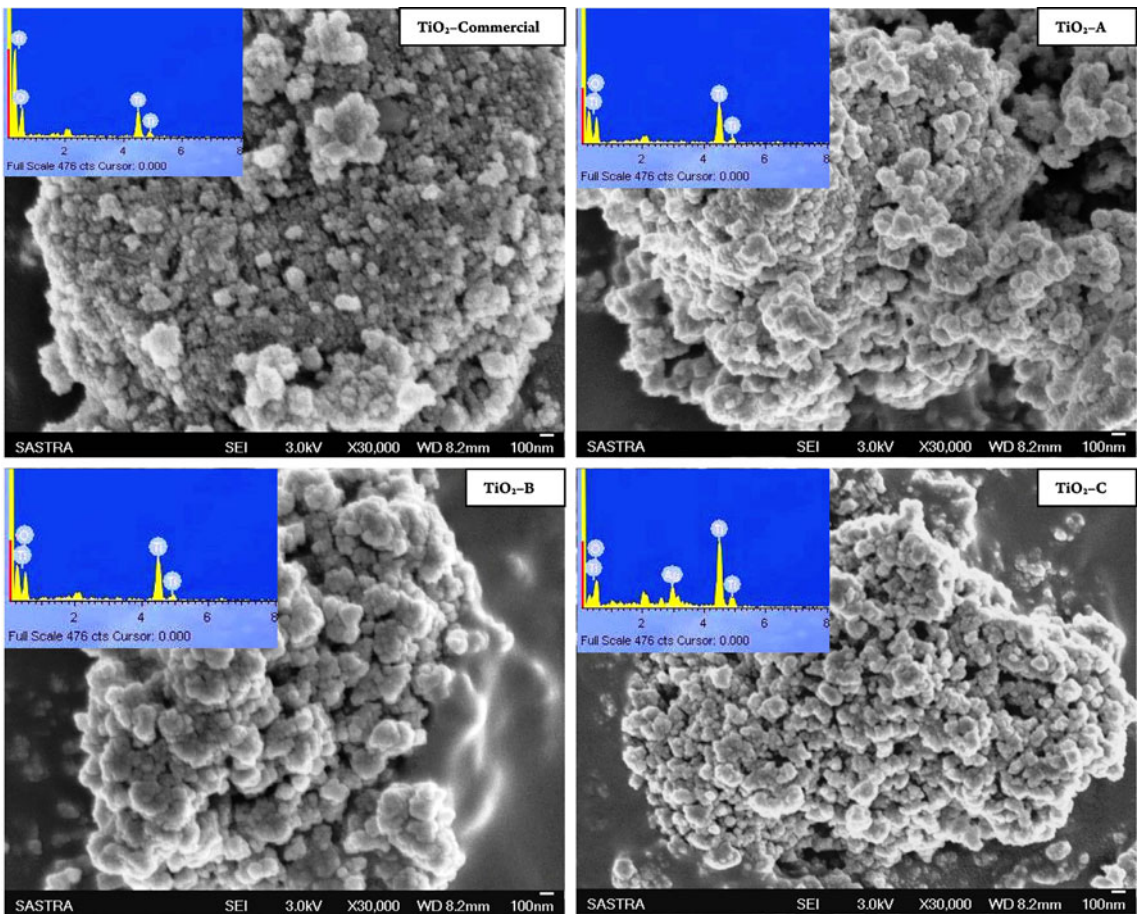

Fig. 2 UV–Vis absorbance measurements for TiO_2-A, TiO_2-B and TiO_2-C

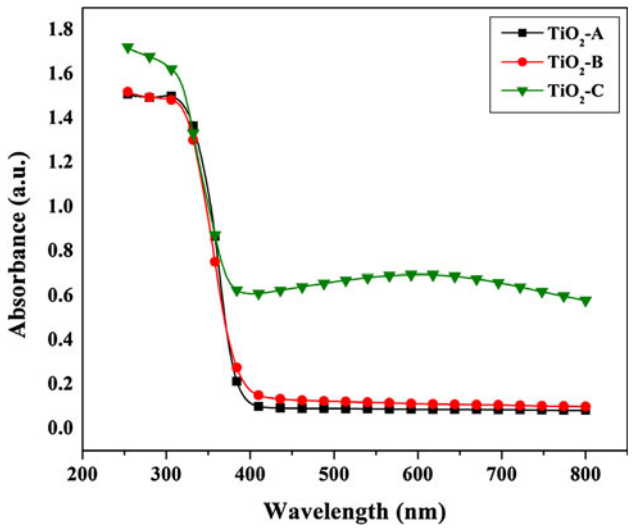

Fig. 3 SEM and EDX (*inset*) images of TiO_2-Commercial, TiO_2-A, TiO_2-B, and TiO_2-C

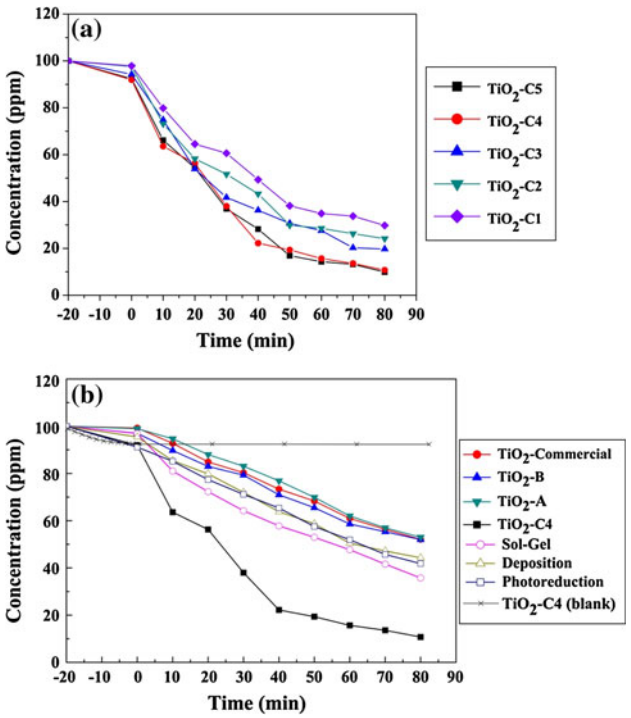

Fig. 4 **a** Photodegradation using biotemplated Ag doped TiO_2-C (where C1, C2, C3, C4 and C5 corresponds to 1–5 mol% Ag). Dye concentration = 100 ppm, catalyst concentration = 1 g/l. **b** Photodegradation of reactive *black* using TiO_2-C4 in comparison with TiO_2-A, TiO_2-B and TiO_2-Commercial and TiO_2 prepared by sol–gel, photodegradation, deposition and TiO_2-C4 blank (*dark* adsorption). Dye concentration = 100 ppm, catalyst concentration = 1 g/l

resulted in formation of secondary particles by self-assembly and epitaxial growth of primary particles [32]. Size of particles as determined from XRD and SEM analysis is given in Table 1. These sizes correspond to crystallite size and grain size respectively. A grain is formed by agglomeration of several crystallites. Presence of titanium, oxygen and silver was confirmed from the elemental analysis of energy-dispersive spectroscopy (EDS) shown as inset in SEM images.

The surface area and pore size measurements were measured with N_2 gas at 77.3 K. From Table 1 it was observed that TiO_2-B had maximum surface area among the three samples followed by TiO_2-C. Surface area was lowest for TiO_2-A. The pore size of TiO_2-A, TiO_2-B and TiO_2-C were 19.73, 23.95 and 21.63 nm respectively. Increase in surface areas and pore width of TiO_2-B and TiO_2-C were mainly due to biotemplating. The deposition of silver on the pores of TiO_2 was probably the cause for the difference in surface area between TiO_2-B and TiO_2-C [33].

3.3 Photocatalytic studies

The photocatalytic activities of synthesized materials were analyzed by studying the degradation of commercial reactive black dye under solar irradiation. Decrease in color during photocatalytic oxidation was determined from the optical densities of samples. Biotemplated Ag–TiO_2 samples with 1–5 mol% of silver concentration were synthesized and compared for their photocatalytic activity under solar light irradiation. The comparison is shown in Fig. 4a. TiO_2 samples prepared with higher silver concentration in the synthesis solution had shown better decolorization kinetics. One-way ANOVA was performed to study the influence of silver nitrate concentration used in the synthesis and the results are shown in Table 2. Results confirmed that the silver nitrate concentration had statistically significant ($p < 0.05$) effect on the photocatalytic activity of the samples. Further, Tukey test was performed to test the null hypothesis (H0: equal means) and it was found that the means for TiO_2-C4 and TiO_2-C5 were not statistically different ($p > 0.05$).

Subsequently, TiO_2-C4 was further compared with TiO_2-Commercial, TiO_2-A, TiO_2-B and TiO_2 synthesized by other methods like solgel, deposition and photoreduction. The comparison shown in Fig. 4b. It was evident from the figure that incorporation of silver had improved the solar light activity of the sample significantly. However, to confirm this, one-way ANOVA was performed and it was confirmed that there was a statistical difference between the samples ($p < 0.05$) (Table 3). Further, Tukey test confirmed that the photocatalytic efficiency of TiO_2-C4 was statistically different from other samples. Meanwhile, TiO_2-A and TiO_2-B had shown 30 % color removal and their photocatalytic efficiencies were comparable to that of the commercial TiO_2 photocatalyst. The difference between other three samples, TiO_2-A, TiO_2-B and TiO_2-Commercial, were not statistically significant ($p > 0.05$).

Table 2 Statistical analysis for TiO_2-C (with 1–5 mol% Ag)

ANOVA[a]					
Source	DF	SS	MS	F	*p*
Catalyst	4	588.542	147.136	786.92	0
Error	5	0.935	0.187		
Total	9	589.477			

Tukey test[b]			
Catalyst	N	Mean	Grouping
TiO_2-C5	2	90.299	◙
TiO_2-C4	2	89.636	◙
TiO_2-C3	2	80.642	♦
TiO_2-C2	2	75.917	□
TiO_2-C1	2	70.601	◀

[a] $S = 0.4324$, $R^2 = 99.84$ %, R^2 (adj) = 99.71 %

[b] Means that do not share a symbol are significantly different

Table 3 Statistical analysis for different TiO_2 catalysts

ANOVA[a]					
Source	DF	SS	MS	F	*p*
Catalyst	3	2,645.101	881.7	13,113.22	0
Error	4	0.269	0.067		
Total	7	2,645.37			

Tukey test[b]			
Catalyst	N	Mean	Grouping
TiO_2-C4	2	89.636	□
TiO_2-B	2	48.004	♦
TiO_2-Commercial	2	47.956	♦
TiO_2-A	2	46.999	♦

[a] $S = 0.2593$, $R^2 = 99.99$ %, R^2 (adj) = 99.98 %

[b] Means that do not share a symbol are significantly different

Among all the samples tested, Ag–TiO_2 biotemplate material showed superior degradation in solar light (92 % color removal). As discussed in Sect. 3.2 presence of silver in TiO_2-C is confirmed by XRD. Transfer of interfacial electrons and excitation of surface electrons due to surface plasmon resonance of silver [34] are the possible reasons for the increase in solar light activity of the samples. Oxygen vacancy is produced in Ag incorporated TiO_2 materials and silver ions present in TiO_2 acts as electron scavengers and enhance photodegradation under solar light. In order to reveal advantage points of the preparation method using enzyme, Ag–TiO_2 powders were also prepared by photoreduction, sol–gel and deposition methods as described by Sahoo et al. [35], Senthilkumaar et al. [36] and Rupa et al. [37] respectively. The photocatalytic efficiencies of all these samples were compared and the comparison is shown in Fig. 4b. From the figure it can be seen that Ag–TiO_2 prepared by enzymatic method showed superior degradation for higher concentration of dye. It could also be seen that the slope the concentration decay curve significantly changed in the case of TiO_2-C4 when reaction mixture was exposed to sun light. It suggested that the TiO_2-C4 sample possessed good activity in the solar range. For other samples the slope of the curve did not change appreciably. Further to elucidate the difference between adsorption and photodegradation, a blank experiment (dark experiment) was included for the sample TiO_2-C4. It can be seen that the adsorption equilibrium was attained with in 25 min approximately. At adsorption equilibrium the percentage color removal was about 10 % while the color removal up to 90 % was achieved by photodegradation. With initial dye concentration of 100 mg/l, equilibrium dye uptake was 9 mg/g of catalyst under dark condition. However, with same initial dye concentration (100 mg/l) upon exposure of solar light 89 mg of dye was removed per g of catalyst after 80 min. This observation confirmed that silver modified TiO_2 had solar activity.

4 Conclusions

Three different types of TiO_2 samples (1) TiO_2 by conventional sol–gel method (TiO_2-A,); (2) TiO_2 using *E. coli* as biotemplate (TiO_2-B); and (3) Ag–TiO_2 using *E. coli* as biotemplate (TiO_2-C) were synthesized using eco-friendly method with an objective to produce solar light active TiO_2. The synthesized materials were characterized for their morphology and chemical composition. The XRD and XRF data revealed the presence of anatase phase TiO_2 and silver in synthesized material. From SEM, the morphology was found as clusters of nano spherical grains. EDS confirmed the presence of titanium, oxygen and silver through the elemental analysis. Activity shift to visible region due to incorporation of silver ions on TiO_2 was confirmed from UV–Vis absorption spectra. From the results, it was shown that the enzyme mediated synthesis reported in the study was effective and significantly improved the photocatalytic efficiencies of the sample. Thus, the proposed method of enzyme mediated in situ synthesis of Ag–TiO_2 with *E. Coli* as biotemplate appears to be an attractive eco-friendly synthesis of solar light active TiO_2 photocatalyst.

Acknowledgments The authors acknowledge SASTRA University for providing financial assistance through Prof. T. R. Rajagopalan research fund. The authors also thank Department of Science and Technology, Government of India for providing access to Surface

Area Analyzer through Grant No: VI-D&P/267/08/09/TDT of Drugs and Pharmaceutical Research Programme.

References

1. Schulte AJ, Koch K, Spaeth M, Barthlott W (2009) Biomimetic replicas: transfer of complex architectures with different optical properties from plant surfaces onto technical materials. Acta Biomater 5:1848–1854
2. Meyers MA, Chen P-Y, Lopez MI, Seki Y, Lin AYM (2011) Biological materials: a materials science approach. J Mech Behav Biomed Mater 4:626–657
3. Ravindran A, Chandran P, Khan SS (2013) Biointerfaces biofunctionalized silver nanoparticles: advances and prospects. Colloids Surf B Biointerfaces 105:342–352
4. Gunasekar V, Gowdhaman D, Ponnusami V (2013) Biodegradation of reactive red M5B dye using *Bacillus subtilis*. Int J ChemTech Res 5:131–135
5. Ponnusami V, Gunasekar V, Srivastava SN (2009) Kinetics of methylene blue removal from aqueous solution using gulmohar (*Delonix regia*) plant leaf powder: multivariate regression analysis. J Hazard Mater 169:119–127
6. Anjaneyulu Y, Sreedhara Chary N, Raj DSS (2005) Decolourization of Industrial effluents—available Methods and emerging technologies—a review. Rev Environ Sci Biotechnol 4:245–273
7. Laasri L, Khalid Elamrani M, Cherkaoui O (2007) Removal of two cationic dyes from a textile effluent by filtration-adsorption on wood sawdust. Environ Sci Pollut Res Int 14:237–240
8. Trujillo-Reyes J, Solache-Ríos M, Vilchis-Nestor A, Sánchez-Mendieta V, Colín-Cruz A (2012) Fe–Ni nanostructures and C/Fe–Ni composites as adsorbents for the removal of a textile dye from aqueous solution. Water Air Soil Pollut 223:1331–1341
9. Beltrán-Heredia J, Sánchez-Martín J, Jiménez-Giles M (2011) Tannin-based coagulants in the depuration of textile wastewater effluents: elimination of anthraquinonic dyes. Water Air Soil Pollut 222:53–64
10. Selvakumar S, Manivasagan R, Chinnappan K (2013) Biodegradation and decolourization of textile dye wastewater using *Ganoderma lucidum*. 3 Biotech 3:71–79
11. Gümüş D, Akbal F (2011) Photocatalytic degradation of textile dye and wastewater. Water Air Soil Pollut 216:117–124
12. Allen DW, Kartal N, Acar F, Sökmen M, Allen DW, Akkaş F, Kartal N, Acar F (2001) Photo-degradation of some dyes using Ag-loaded titaniumdioxide. Water Air Soil Pollut 132:153–163
13. Sanoop PKK, Anas S, Ananthakumar S, Gunasekar V, Saravanan R, Ponnusami V (2012) Synthesis of yttrium doped nanocrystalline ZnO and its photocatalytic activity in methylene blue degradation. Arab J Chem. doi:10.1016/j.arabjc.2012.04.023
14. Mills A, Le Hunte S (2000) An overview of semiconductor photocatalysis. J Photochem Photobiol A 108:1–35
15. Hoffmann MR, Martin ST, Choi W, Bahnemannt DW (1995) Environmental applications of semiconductor photocatalysis. Chem Rev 95:69–96
16. Chakrabarti S, Dutta BK (2004) Photocatalytic degradation of model textile dyes in wastewater using ZnO as semiconductor catalyst. J Hazard Mater 112:269–278
17. Fujishima A, Zhang X, Tryk D (2008) Titanium dioxide photocatalysis. J Photochem Photobiol C 1:1–21
18. Rahimi R, Honarvar E (2012) Degradation of methylene blue via Co–TiO_2 nano powders modified by meso-tetra (carboxyphenyl) porphyrin. J Sol–Gel Sci Technol 62:351–357
19. Rehman S, Ullah R, Butt AM, Gohar ND (2009) Strategies of making TiO_2 and ZnO visible light active. J Hazard Mater 170:560–569
20. Fujishima A, Zhang X, Tryk D (2008) TiO_2 photocatalysis and related surface phenomena. Surf Sci Rep 63:515–582
21. Singh D, Singh N, Dutta S (2011) Bandgap modification of TiO_2 sol–gel films by Fe and Ni doping. J Sol–Gel Sci Technol 58:269–276
22. Shen Y, Xiong T, Du H, Jin H, Shang J, Yang K, Photocatalysis VÁ (2009) Phosphorous, nitrogen, and molybdenum ternary co-doped TiO_2: preparation and photocatalytic activities under visible light. J Sol–Gel Sci Technol 4:98–102
23. Borlaf M, Poveda JM, Moreno R, Colomer MT (2012) Synthesis and characterization of TiO_2/Rh^{3+} nanoparticulate sols, xerogels and cryogels for photocatalytic applications. J Sol–Gel Sci Technol 63:408–415
24. Luo M, Gao J, Zhang X, Yang J, Hou G, Ouyang D, Jin Z (2007) Processing of porous TiN/C ceramics from biological templates. Mater Lett 61:186–188
25. Dong Q, Su H, Zhang D, Liu Z, Lai Y (2007) Synthesis of hierarchical mesoporous titania with interwoven networks by eggshell membrane directed sol–gel technique. Microporous Mesoporous Mater 98:344–351
26. Zhang W, Zhang D, Fan T, Ding J, Guo Q, Ogawa H (2006) Morphosynthesis of hierarchical ZnO replica using butterfly wing scales as templates. Microporous Mesoporous Mater 92:227–233
27. Chang L, Wei LI-C, Audia JP, Morton RA, Schellhorn HE (1999) Expression of the *Escherichia coli* NRZ nitrate reductase is highly growth phase dependent and is controlled by RpoS, the alternative vegetative sigma factor. Mol Microbiol 34:756–766
28. Anil Kumar S, Abyaneh MK, Gosavi SW, Kulkarni SK, Pasricha R, Ahmad A, Khan MI (2007) Nitrate reductase-mediated synthesis of silver nanoparticles from $AgNO_3$. Biotechnol Lett 29:439–445
29. Suwanchawalit C, Wongnawa S, Sriprang P, Meanha P (2012) Enhancement of the photocatalytic performance of Ag-modified TiO2 photocatalyst under visible light. Ceram Int 38:5201–5207
30. Kalishwaralal K, Deepak V, Ramkumarpandian S, Nellaiah H, Sangiliyandi G (2008) Extracellular biosynthesis of silver nanoparticles by the culture supernatant of *Bacillus licheniformis*. Mater Lett 62:4411–4413
31. Gurunathan S, Kalishwaralal K, Vaidyanathan R, Venkataraman D, Pandian SRK, Muniyandi J, Hariharan N, Eom SH (2009) Biosynthesis, purification and characterization of silver nanoparticles using *Escherichia coli*. Colloids Surf B 74:328–335
32. Mitchell CEJ, Howard A, Carney M, Egdell RG (2001) Direct observation of behaviour of Au nanoclusters on TiO_2 (110) at elevated temperatures. Surf Sci 490:196–210
33. Sakthivel S, Shankar MV, Palanichamy M, Arabindoo B, Bahnemann DW, Murugesan V (2004) Enhancement of photocatalytic activity by metal deposition: characterisation and photonic efficiency of Pt, Au and Pd deposited on TiO_2 catalyst. Water Res 38:3001–3008
34. Khan Z, Al-Thabaiti SA, Obaid AY, Al-Youbi AO (2011) Preparation and characterization of silver nanoparticles by chemical reduction method. Colloids Surf B 82:513–517
35. Sahoo C, Gupta AK, Pal A (2005) Photocatalytic degradation of Methyl Red dye in aqueous solutions under UV irradiation using Ag^+ doped TiO_2. Desalin 181:91–100
36. Senthilkumaar S, Porkodi K, Gomathi R, Maheswari AG, Manonmani N (2006) Sol–gel derived silver doped nanocrystalline titania catalysed photodegradation of methylene blue from aqueous solution. Dyes Pigment 69:22–30
37. Rupa AV, Manikandan D, Divakar D, Sivakumar T (2007) Effect of deposition of Ag on TiO_2 nanoparticles on the photodegradation of reactive yellow-17. J Hazard Mater 147:906–913